Available online at www.sciencedirect.com

ScienceDirect

journal homepage: www.elsevier.com/locate/he

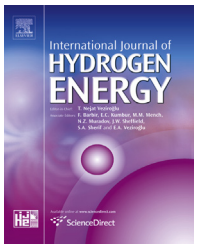

Solvent effect on the Nafion agglomerate morphology in the catalyst layer of the proton exchange membrane fuel cells

Tae-Hyun Kim [a], *Jae-You Yi* [a], *Chi-Young Jung* [b], *Euigyung Jeong* [c], *Sung-Chul Yi* [a,d,*]

[a] *Department of Chemical Engineering, Hanyang University, Seoul 133-791, Republic of Korea*
[b] *Hydrogen & Fuel Cell Center, New & Renewable Energy Research Division, Korea Institute of Energy Research (KIER), Buan-gun 579-841, Republic of Korea*
[c] *The 4th R&D Research Institute, Agency for Defense Development, Daejeon 305-600, Republic of Korea*
[d] *Department of Hydrogen and Fuel Cell Technology, Hanyang University, Seoul 133-791, Republic of Korea*

ARTICLE INFO

Article history:
Received 12 March 2016
Received in revised form
21 November 2016
Accepted 5 December 2016
Available online 22 December 2016

Keywords:
Proton exchange membrane fuel cell
Membrane electrode assembly
Catalyst ink
Nafion mobility

ABSTRACT

In this work, we investigated the influence of the solvents used in the catalyst ink on performance of the proton exchange membrane fuel cells (PEMFCs). The mobility of the polymeric chains in 2.5 wt% Nafion dispersion is measured by fluorine-19 nuclear magnetic resonance after the use of different organic solvents including isopropyl alcohol (IPA), dimethyl sulfoxide (DMSO) and N-Methyl-2-pyrrolidone (NMP). Subsequently, the electrochemical properties, e.g., direct-current polarization and electrochemical impedance spectra, are characterized. As a result, the catalyst layer fabricated from the solvents with high main-chain mobility created more intimate contact at triple-phase boundary, enlarging the electrochemically available surface area and reducing the charge-transfer resistance, mainly due to a strong interaction between solvent molecule and Nafion ionomer. It is demonstrated that the use of the membrane electrode assemblies (MEAs) fabricated from NMP- and DMSO-based catalyst inks enable a H_2/O_2 PEMFC to yield 100% and 33% higher power densities at 0.6 V, respectively, as compared to the MEA fabricated from IPA-based catalyst ink.

Introduction

The proton exchange membrane fuel cells (PEMFCs) are one of highly efficient electrochemical energy conversion technologies, with the potential to replace the conventional fossil-fueled power generators for the vehicle and stationary applications. Despite the ever-increasing efforts, several remaining challenges involved with performance, cost and durability must first be addressed [1]. In particular, the catalyst layer (CL) consists of the carbon-supported platinum (Pt/C) catalyst, Nafion binder and pore pathway (reactant species), which play a key role in formation of the triple-phase boundary (TPB) and significantly affect the electrode kinetics. Hence, the optimization of the catalyst ink composition is imperative to achieve

*Corresponding author. Department of Chemical Engineering, Hanyang University, Seoul 133-791, Republic of Korea. Fax: +82 2 2298 5147.
E-mail address: scyi@hanyang.ac.kr (S.-C. Yi).
http://dx.doi.org/10.1016/j.ijhydene.2016.12.015
0360-3199/

an improved performance for the resultant membrane electrode assembly (MEA) [2].

A number of research groups have extensively investigated the effect of the catalyst ink composition on the fuel-cell performance [3–38]. Initially, the Nafion ionomer loaded in the CL has been spotlighted because it serves as both polymeric binder and proton conductor [3–7]. Optimal value for the Nafion and corresponding catalyst loadings are found to be essential in achieving higher performance. An excessive amount of Nafion may increase the mass-transport resistance or poison the catalytic surfaces, while deficient Nafion mass loading decreases the proton conductivity of CL or the TPB area [3,5]. Meanwhile, the attempts to efficiently reduce the platinum (Pt) loading have involved how to improve the electrode's surface utilization [8–23]. Typically, the MEAs can be fabricated by the catalyst-coated membrane or catalyst-coated gas diffusion layer methods. The techniques to prepare the MEAs include spraying, electrospraying, ultrasonic-spraying, decal transfer, screen-printing or brushing methods [8–16]. To maximize the TPB in the CL, numerous studies have been extensively conducted on optimization of the fabrication processing parameters such as hot-pressing conditions, annealing temperature, or decal substrates [17–23]. Although the CL fabrication in the state-of-the-art PEMFC lowered the mass loading under 0.2 mg_{Pt} cm^{-2}, further reduction of Pt is still required to succeed in commercialization [24]. There have been thus intensive researches focusing on the CL fabrication with a suitable porous structure for the improved polarization [25–31]. Uchida et al. firstly explored the effect of dielectric constant (ε) on the degree of Nafion agglomeration, by classifying organic solvents into three different categories, i.e., solution ($\varepsilon > 10$), colloid ($3 < \varepsilon < 10$) and precipitation ($\varepsilon < 3$) [32]. Inspired by them, Shin et al. investigated the CL structure and electrochemical properties by employing normal-butyl acetate ($\varepsilon = 5.01$) and isopropyl alcohol (IPA) ($\varepsilon = 18.3$) as the colloid and solvent type catalyst ink, respectively [33]. The CLs prepared by the colloidal method presented higher porosity, with pore diameters between 0.02 and 0.07 μm as compared with the solution method. They suggested that the colloidal type ink is beneficial in creating highly porous CL structure and thereby achieving reduced mass-transport resistance and ohmic resistance. Since then, researchers have investigated the solvent effect on the fuel-cell performance based on the ε and/or thermodynamic properties of solvents with various MEA-fabrication techniques [34–38]. In order to ensure the reliability, they conducted pretreatment of the Nafion membrane and post-treatment of the MEAs which were previously reported [9–11,39–41]. Exceptional cases have been reported that the MEAs fabricated from ethylene glycol ($\varepsilon = 38.66$) and cyclohexanol ($\varepsilon = 15.0$) based inks showed higher performance than that of the MEAs produced from ethylene glycol dimethyl ether ($\varepsilon = 7.20$) and diethyl oxalate ($\varepsilon = 8.10$) based inks. Therefore, the key solvent property for the catalyst ink, that is decisive on the fuel-cell performance, is still lacking.

More accurate measurement of the physicochemical properties in the CL has attracted many of us into further exploration. Several researchers have conducted the thin-film confinement experiments to evaluate more realistic values for the CL properties as the thickness of the Nafion layer covering the Pt/C aggregates is severely reduced by three orders of magnitude as compared to the Nafion membrane [42–47]. They found that the water uptake drastically increased when the thickness of Nafion layer was confined below 50 nm, while the proton conductivity decreased [44]. This may be attributed to weakly assembled and poorly interconnected water channels in such a thin Nafion layer. Hence, thin Nafion layer in the CL may provide further limitations exceeding our expectations. It is also reported that various organic solvents exhibit different mobilities of the Nafion ionomer, thereby resulting in different morphologies of the Nafion agglomerates and eventually affecting the CL structures [48–53]. Recently, Kim et al., for the first time, evidenced that the interface between the Nafion ionomer and solvent molecule in the catalyst ink may be critical for both performance and durability of the PEMFCs due to variation of mechanical properties resulted from different mobilities of Nafion ionomer [52,53]. Yet, the mobilities of the main chain and side chain in various solvents, as well as their impacts on the fuel cell performance, should be investigated separately, considering the chemical structure of Nafion consisting of distinct hydrophilic and hydrophobic domains.

As discussed, the dispersion states and degrees of agglomeration in the catalyst ink are strongly dependent on the mobilities of Nafion. In this work, we investigated the influence of the dispersing solvents which differ in the main-chain mobility of Nafion, for it exhibits a large impact on the morphology of the Nafion agglomerates and may not severely affect several key properties, such as water uptake and proton conductivity. For purpose of comparison, all the CLs are annealed at a fixed evaporation rate of 4.5 wt% min^{-1} in course of the modified decal transfer method [6]. Subsequently, the CL microstructures and their impacts on the cell polarization are explored. The electrochemical properties of the CLs are further evaluated by the cyclic voltammetry (CV) and electrochemical impedance spectroscopy (EIS).

Experimental

Preparation of the membrane electrode assembly

The catalyst ink was prepared by mixing 0.11 g of the Pt/C catalyst (HiSPEC 3000, Alfa Aesar) and 1.232 g of the 5 wt% Nafion dispersion (DE521, Ion Power) into 1.296 g of solvent. Here, IPA, dimethyl sulfoxide (DMSO) and N-methyl-2-pyrrolidone (NMP) were purchased from Sigma Aldrich to use as the solvent. Prior to homogenization, 0.06 g of tetrabutylammonium hydroxide (40 wt%, Alfa Aesar) was added to change the protonated Nafion to the TBA-form Nafion in order to provide sufficient viscosity to the catalyst ink.

The MEAs fabricated from different solvents were prepared in the same manner as follow. The ink was repeatedly painted onto the polytetrafluoroethylene (PTFE) sheet and annealed in a convection oven until the Pt loading reached 0.2 mg cm^{-2} (four-times painted on the decal). Not only to rule out the effect of evaporation rate but also to prevent the formation of cracks on the CLs, the evaporation rate of solvent was controlled to be constant, about 4.5 wt% min^{-1} in average (90 wt% on 20 min), through the annealing process, with

varying the annealing temperatures of 25, 50 and 90 °C for IPA, DMSO and NMP, respectively [6,54,55]. Subsequently, the CL absorbed by 1-propanol was transferred to the sodium-form Nafion membrane (NRE212, DuPont) by hot-pressing method at 60 °C for 10 min [56,57]. The MEA was boiled in deionized water at 100 °C to remove residual solvent in the CL. After that, the MEA was immersed in 0.5 M sulfuric acid solution at 70 °C to change the TBA- or sodium-form Nafion into the protonated Nafion, followed by cleansing in the boiling water. The resulting MEA was wiped and dried for 1 h in vacuum oven before characterizations.

Characterization

The fluorine-19 nuclear magnetic resonance (^{19}F NMR) (Avance-300) was conducted at 282.4 MHz to obtain the mobility of Nafion dispersed in different solvents which have 2.5 wt% Nafion content [50]. The field-emission scanning electron micrograph (SEM) analysis (JSM-6330F) was implemented using the MEA to obtain the surface morphology of the CL. The CL morphology was further examined in perspective of the phase separation by the tapping-mode atomic force microscopy (AFM) (XE 100). To clearly observe the phase-separated morphology, the MEA sample was dried in a vacuum oven at 50 °C for 2 h and then pretreated in the 30% relative-humidity nitrogen flow at room temperature for 24 h.

The fuel-cell performance was measured with a 9 cm^2 three-serpentine cell fixture at 70 °C and ambient pressure. The fully-humidified feed gases were supplied into the cell at 150 sccm for the hydrogen anode and the oxygen cathode. The electrochemical impedance spectroscopy (EIS) was measured at 70 °C by a potentiostat/galvanostat working as an impedance analyzer (Gamry Reference 3000). After stabilizing the MEA at 0.8 V for 20 min, the impedance spectra were recorded at 0.8 V with a voltage perturbation of 0.27 mV at frequencies ranging from 20,000–0.1 Hz. For the cyclic voltammetry (CV), the hydrogen and nitrogen feeds were supplied to the cell at 20 sccm and 9 sccm, respectively, while the cell and the humidification temperature was maintained at 30 °C. The low nitrogen flow rate was applied to avoid excessive hydrogen evolution reaction [57]. The potential was cycled from 0.05 to 1.20 V at a scan rate of 50 mV s^{-1}. The charge involved in hydrogen adsorption was used to calculate the electrochemical surface area (ECSA) after correcting the influence of double-layer charging/discharging and hydrogen evolution.

Results and discussion

Mobility of the Nafion ionomer in organic solvents

As illustrated in Fig. 1, the Nafion ionomer consists of the hydrophobic PTFE main chain and hydrophilic sulfonic-acid side chain. The Pt/C-Nafion agglomerates are formed through the secondary agglomeration of the primary Pt/C-Nafion agglomerates (in size of 100–300 nm) [58]. During the process, the solvent–Nafion interaction becomes more determinant factor in the wettability of the Pt/C-Nafion agglomerates than the solvent–catalyst interaction because of the Nafion layer covering the agglomerates [58,59]. The CL structures, particularly the morphology of the Pt/C catalyst and Nafion agglomerates, thereby depend on mobilities of the main chains and side chains of Nafion in the catalyst ink, which may be further affected by the dispersing solvents. The Nafion ionomer dispersed in the solvents with higher mobility is projected to have relatively weaker clustering behavior and smaller agglomerated structures due to higher degrees of the phase separation. Recently, Los Alamos National Laboratory reported that the Nafion ionomer dispersed in NMP, a well-known solvent for the ability to solubilize various types of polymers, presented its agglomerated unit structure smaller than 10 nm [50,53]. Thus, in case of the catalyst ink for PEMFCs, the Nafion agglomerates in NMP may penetrate deeply into the aggregated Pt/C catalysts, not only enlarging the contact area at TPB but also thinning the Nafion layer covering the Pt/C aggregates.

Fig. 2 shows the mobility of the Nafion ionomer dispersed in different solvents, namely, IPA, DMSO and NMP. The mobility was evaluated based on the ^{19}F NMR spectra which are presented in Fig. 2a. All peaks in the spectra were marked with the labeled fluorine types of sodium-form Nafion. The Nafion dispersed in water was employed as a benchmark data, as water is included in the commercial Nafion dispersion purchased and always involved in the catalyst ink during the CL fabrication process. The Nafion mobility can be qualitatively analyzed by comparing the sharpness of peaks. The spectra of NMP and DMSO show sharper peak at approximately 122 ppm than that of IPA which indicates higher mobility of the main chain. However, it is difficult to compare the mobilities of both the main chain and side chain from the peaks in Fig. 2a. To quantitatively compare the mobility of Nafion dispersed in different solvents, the degrees of the Nafion mobility have often been evaluated by the intensity area and/or line width of the peaks [50,60,61]. The mobilities of the main chain and side chain were calculated as described in equations (1) and (2) [49].

$$\text{Relative main chain mobility} = \frac{\text{Peak area of 1}}{\text{Peak area of 3, 5, 6}} \quad (1)$$

$$\text{Side chain mobility} = \frac{1}{\text{Line width of peak 3, 5, 6}} \quad (2)$$

In Fig. 2b, the side-chain mobilities of Nafion dispersed in the solvents showed sufficiently high and similar values above 1.5 kHz^{-1} (1.725, 1.539 and 1.789 kHz^{-1} for IPA, DMSO and NMP, respectively). However, the Nafion ionomers dispersed in DMSO and NMP presented considerably higher mobility for the main chain as compared with IPA. The higher mobility indicates stronger interaction between the solvent molecules and main chain of Nafion, which is consistent with the small angle neutron scattering data reported by Welch et al. [50], and thus implies further segregation between the hydrophilic and hydrophobic domains. This weaker clustering behavior of Nafion may develop more invasive and separated morphologies for the Pt/C-Nafion agglomerates, hence leading to a significant improvement on the fuel-cell performance.

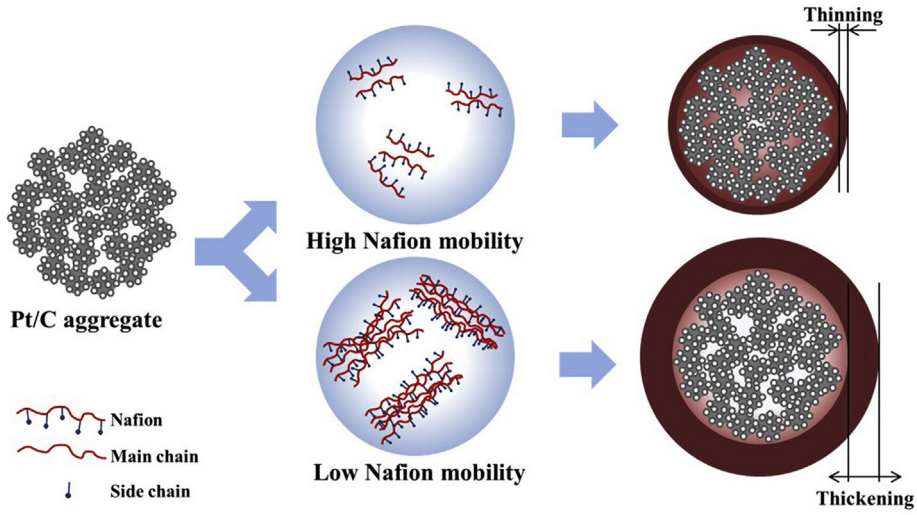

Fig. 1 – Schematic illustration of the effect of the Nafion mobility on the Pt/C-Nafion agglomerate structure.

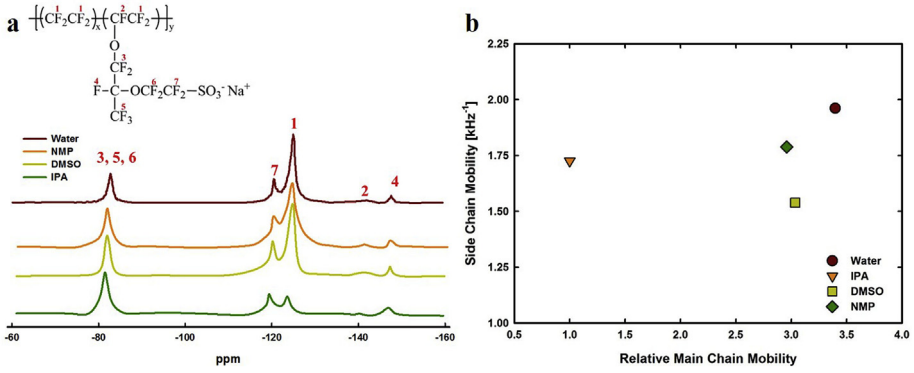

Fig. 2 – a: Chemical structure of sodium-form Nafion with labeled fluorine types and ^{19}F NMR spectra of the Nafion ionomer with different solvents, b: Plot of the mobility of the Nafion ionomer dispersed in various solvents.

Morphology of the catalyst layer

The CL structure was investigated to examine the impact of the Nafion mobility, as the agglomerated structure of Nafion dispersed into the solvent retains its characteristic morphology and affects the final morphology of the CL [53,62]. Fig. 3 shows the SEM images of the CL surfaces fabricated from different organic solvents. As can be seen in Fig. 3, the CL fabricated from the catalyst inks consisting of the solvents with higher main-chain mobility, such as DMSO and NMP, showed finer agglomerates when compared to the CL made from IPA. Especially, the NMP CL presented evenly-distributed and less-clustered morphology, with the densest structure among all the CLs. Due to higher side-chain mobility in NMP compared to that of DMSO, the NMP CL could be exhibited notably finer agglomerate structure than the DMSO CL. However, the CL fabricated from the IPA-based catalyst ink showed largely-aggregated structure because of the low main-chain mobility of Nafion.

Typically, the CLs consist of pores with diameters of up to 40 nm inside the Pt/C aggregates and 40–1000 nm among the aggregates, which are referred to as the primary and

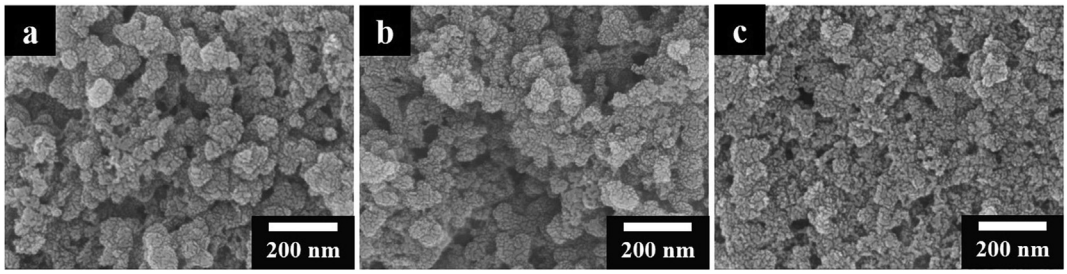

Fig. 3 – SEM images of the surface of CL prepared by different solvents. a: IPA, b: DMSO and c: NMP.

secondary pores, respectively [63]. The Nafion agglomerates dispersed in the solvent with low main-chain mobility, in size of 300–350 nm [50,53], may contact the outer surfaces of the Pt/C aggregates rather than deeply penetrate into the central parts, while the solvents with high main-chain mobility enable Nafion permeate through the Pt/C aggregates due to the reduced agglomerate size (smaller than 10 nm in case of NMP [50,53]) resulted from a severe phase separation. Hence, the less-clustered Pt/C-Nafion agglomerate prepared by the solvent with high main-chain mobility presented the dense and fine microstructure. In addition, thin Nafion layer covering larger surface area of the Pt/C aggregates can be fabricated in the CLs made from the solvents with high main-chain mobility. It can be deduced, from the SEM images, that the solvent's ability to mobilize the Nafion ionomer significantly influences the CL structures.

Fig. 4 presents the phase images of the CLs obtained by tapping-mode AFM. In the figure, the parts of the CL that are located nearby sulfonic-acid groups and thus more hydrophilic exhibit darker colors because the phase signals lag differently along the water-sorption behaviors. As the Nafion ionomer largely aggregates in the catalyst ink, the image would present aggregated dark or bright colors. Thereby, the distribution of the Nafion ionomer in the Pt/C-Nafion agglomerate could be detected through the AFM images of the CLs. As observed in Fig. 4a, the CL prepared from the IPA-based catalyst ink showed largely-aggregated hydrophobic domains due to the low main-chain mobility of Nafion; however, the CLs fabricated from the solvents with high main-chain mobility exhibited well-separated boundaries between the hydrophilic and hydrophobic domains. Moreover, the NMP CL showed remarkably highly-separated hydrophilic–hydrophobic domain compared to that of the DMSO CL owing to its finer agglomerate structure compared to that of the DMSO CL. As a consequence, the NMP-based catalyst ink led to the fabrication of the CLs, composed of well-connected and evenly-distributed hydrophilic–hydrophobic domains, having densely-packed structures with a shallow coverage of Nafion. It is therefore highly consistent with the provided SEM images that the catalyst inks based on the solvents with higher main-chain mobility allow more invasive access of Nafion to the Pt surfaces inside the Pt/C aggregates and hence increase the surface area involved in the TPB.

Electrochemical performances

Fig. 5 shows the cell polarizations of the MEAs fabricated from different organic solvents. As observed in the figure, the MEAs prepared from the solvents with high main-chain mobility (NMP and DMSO) exhibited dramatic improvements compared with that made from the solvent with low main-chain mobility (IPA). Specifically, the MEA fabricated from the NMP-based catalyst ink exhibited the highest performance at low-current densities below 0.2 A cm^{-2}. The improvement in the catalytic-activation polarization is attributed to facilitated electrode kinetics; the evenly-distributed hydrophilic and hydrophobic domains on the CL made from the NMP-based catalyst ink may have reduced the catalytic-activation polarization due to intimate contact between Pt and Nafion. At intermediate-current densities, the MEAs fabricated from the DMSO- and NMP-based catalyst inks showed 0.616 A cm^{-2} and 0.925 A cm^{-2} at 0.6 V, respectively, which are 33% and 100% higher than that of the MEA produced from the IPA-based catalyst ink (0.461 A cm^{-2}). The CLs prepared from the solvents with higher main-chain mobility improved the ohmic polarization owing to much densely-packed microstructure on the Pt/C-Nafion agglomerates and thinner Nafion layer sur-

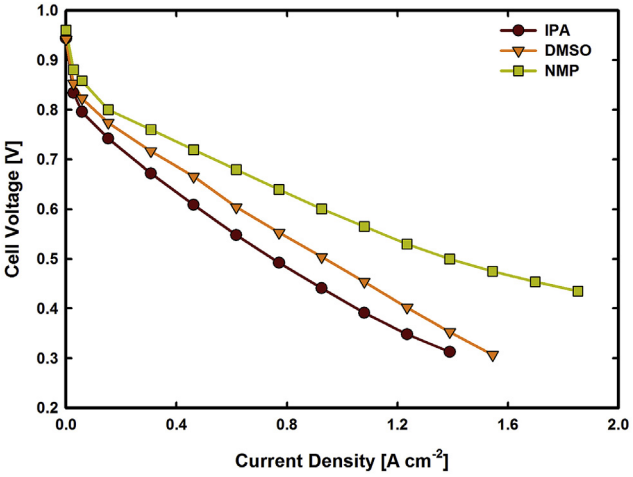

Fig. 5 – Cell polarization of the MEAs prepared from various solvents.

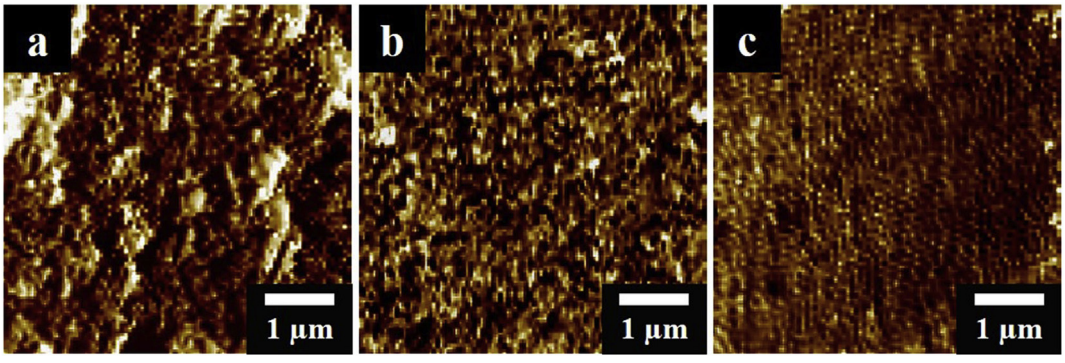

Fig. 4 – AFM images of the surface of CL prepared by different solvents. a: IPA, b: DMSO and c: NMP.

rounding them. Hence, the morphological characteristics of the CLs fabricated from the solvents with higher main-chain mobility may have enlarged the TPB area and improved charge-transfer characteristics through the Nafion covering layer. Therefore, the CV and EIS experiments were further employed to investigate the relation between the CL structure and electrochemical performance.

Fig. 6 shows the CV plots of the MEAs fabricated from different organic solvents to evidence the actual coverage of the Nafion ionomer on the Pt surfaces. The MEA prepared from the IPA-based catalyst ink presented the lowest ECSA of 40.9 $m^2 g^{-1}$. In contrast, the MEAs fabricated from the DMSO- and NMP-based catalyst inks showed rises in the ECSA to 43.0 $m^2 g^{-1}$ and 52.2 $m^2 g^{-1}$, respectively, presenting larger TPB area than that of the MEA prepared from the IPA-based catalyst ink. One possible explanation is that the Nafion ionomer dispersed in the solvents with higher main-chain mobility induce deeper penetration into the Pt/C aggregates to have larger Pt surfaces in contact with Nafion, thereby enhancing the catalytic-activation performance at the low-current densities.

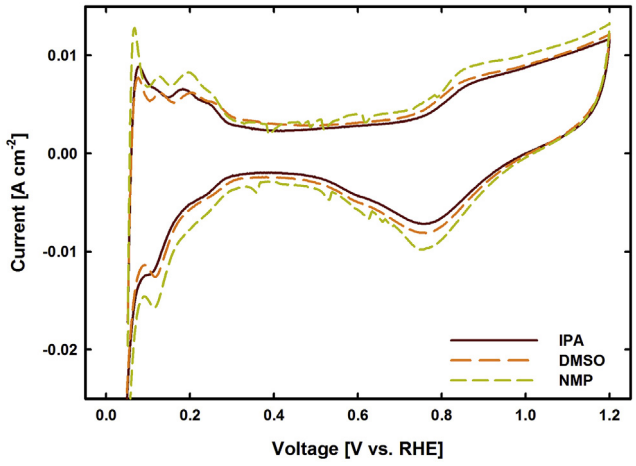

Fig. 6 – Cyclic voltammetry of the MEAs prepared from various solvents.

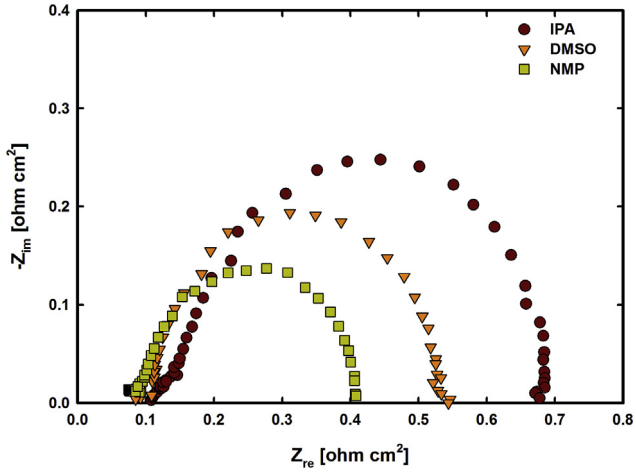

Fig. 7 – Electrochemical impedance data of the MEAs prepared from various solvents at 0.8 V.

Fig. 7 presents the impedance spectra of the MEAs prepared from different solvents. The MEA made from the IPA-based catalyst ink showed the highest charge-transfer resistance at 0.577 Ω cm^2, while those fabricated from the DMSO- and NMP-based catalyst inks presented lower charge-transfer resistances at 0.432 Ω cm^2 and 0.331 Ω cm^2, respectively. Less clustered Nafion agglomerates resulted from the solvent with the high main-chain mobility consistently reduced the charge-transfer resistance in the CL, for it shortens the diffusion path for the proton transport, though the high-frequency resistance for all the MEAs remained similar at about 0.1 Ω cm^2. Therefore, close contact between the Pt/C aggregates with thin Nafion layer is apparently beneficial in improving the ohmic-activation performance.

Conclusions

This paper reports the effect of the solvents in the catalyst ink on the PEMFC performance. We first have screened the solvents which exhibit similar side-chain mobility but differ in main-chain mobility of the Nafion ionomer, and subsequently fabricated the MEAs via modified decal transfer method. The main-chain mobilities resulted in different morphologies of the CLs, mainly attributing to the variation of the Nafion's percolation behavior. The dense and fine microstructure was obtained from the solvent with high main-chain mobility owing to long penetration depth of the Nafion ionomer into the Pt/C-Nafion agglomerate. From the AFM phase images, the Nafion agglomerate morphology on the CL presented the well-distributed hydrophilic–hydrophobic domains when using the solvent with high main-chain mobility. It is clearly demonstrated that the cell polarizations, after using the solvents with higher main-chain mobility, were gradually improved due to an increase in ECSA and a decrease in the charge-transfer resistance. The solvent with higher main-chain mobility, combined with sufficiently high and constant side-chain mobility, is therefore beneficial for enhancing the electrochemical performance.

Acknowledgements

This work was supported by Defense Acquisition Program Administration and Agency for Defense Development under the contract UD120080GD.

REFERENCES

[1] Wang YJ, Wilkinson DP, Zhang J. Noncarbon support materials for polymer electrolyte membrane fuel cell electrocatalysts. Chem Rev 2011;111:7625–51.
[2] Cheng X, Yi B, Han M, Zhang J, Qiao Y, Yu J. Investigation of platinum utilization and morphology in catalyst layer of polymer electrolyte fuel cells. J Power Sources 1999;79:75–81.
[3] Passalacqua E, Lufrano F, Squadrito G, Patti A, Giorgi L. Nafion content in the catalyst layer of polymer electrolyte fuel cells: effects on structure and performance. Electrochim Acta 2001;46:799–805.

[4] Lai CM, Lin JC, Ting FP, Chyou SD, Hsueh KL. Contribution of Nafion loading to the activity of catalysts and the performance of PEMFC. Int J Hydrogen Energy 2008;33:4132–7.
[5] Velázquez-Palenzuela A, Centellas F, Brillas E, Arias C, Rodríguez RM, Garrido JA, et al. Kinetic effect of the ionomer on the oxygen reduction in carbon-supported Pt electrocatalysts. Int J Hydrogen Energy 2012;37:17828–36.
[6] Jung CY, Kim WJ, Yi SC. Optimization of catalyst ink composition for the preparation of a membrane electrode assembly in a proton exchange membrane fuel cell using the decal transfer. Int J Hydrogen Energy 2012;37:18446–54.
[7] Bonifacio RN, Neto AO, Linardi M. Influence of the relative volumes between catalyst and Nafion ionomer in the catalyst layer efficiency. Int J Hydrogen Energy 2014;39:14680–9.
[8] Ticianelli EA, Derouin CR, Redondo A, Srinivasan S. Methods to advance technology of proton exchange membrane fuel cells. J Electrochem Soc 1988;135:2209–14.
[9] Wilson MS, Gottesfeld S. High performance catalyzed membranes of ultra-low Pt loadings for polymer electrolyte fuel cells. J Electrochem Soc 1992;139:L28–30.
[10] Wilson MS, Gottesfeld S. Thin-film catalyst layers for polymer electrolyte fuel cell electrodes. J Appl Electrochem 1992;22:1–7.
[11] Wilson MS, Valerio JA, Gottesfeld S. Low platinum loading electrodes for polymer electrolyte fuel cells fabricated using thermoplastic ionomers. Electrochim Acta 1995;40:355–63.
[12] Wang ED, Shi PF, Du CY. A novel self-humidifying membrane electrode assembly with water transfer region for proton exchange membrane fuel cells. J Power Sources 2008;175:183–8.
[13] Martin S, Garcia-Ybarra PL, Castillo JL. High platinum utilization in ultra-low Pt loaded PEM fuel cell cathodes prepared by electrospraying. Int J Hydrogen Energy 2010;35:10446–51.
[14] Kim KH, Lee KY, Kim HJ, Cho EA, Lee SY, Lim TH, et al. The effects of Nafion® ionomer content in PEMFC MEAs prepared by a catalyst-coated membrane (CCM) spraying method. Int J Hydrogen Energy 2010;35:2119–26.
[15] Hwang DS, Park CH, Yi SC, Lee YM. Optimal catalyst layer structure of polymer electrolyte membrane fuel cell. Int J Hydrogen Energy 2011;6:9876–85.
[16] Hwang TH, Shen HL, Jao TC, Weng FB, Su A. Ultra-low Pt loading for proton exchange membrane fuel cells by catalyst coating technique with ultrasonic spray coating machine. Int J Hydrogen Energy 2012;37:13872–9.
[17] Frey T, Linardi M. Effect of membrane electrode assembly preparation on the polymer electrolyte membrane fuel cell performance. Electrochim Acta 2004;50:99–105.
[18] Jung HY, Cho KY, Lee YM, Park JK, Choi JH, Sung YE. Influence of annealing of membrane electrode assembly (MEA) on performance of direct methanol fuel cell (DMFC). J Power Sources 2007;163:952–6.
[19] Saha MS, Paul DK, Peppley BA, Karan K. Fabrication of catalyst-coated membrane by modified decal transfer technique. Electrochem Commun 2010;12:410–3.
[20] Cho HJ, Jang H, Lim S, Cho EA, Lim TH, Oh IH, et al. Development of a novel decal transfer process for fabrication of high-performance and reliable membrane electrode assemblies for PEMFCs. Int J Hydrogen Energy 2011;36:12465–73.
[21] Yazhanpour M, Esmaeilifar A, Rowshanzamir S. Effects of hot pressing conditions on the performance of Nafion membranes coated by ink-jet printing of Pt/MWCNTs electrocatalyst for PEMFCs. Int J Hydrogen Energy 2012;37:11290–8.
[22] Mehmood A, Ha HY. An efficient decal transfer method using a roll-press to fabricate membrane electrode assemblies for direct methanol fuel cells. Int J Hydrogen Energy 2012;37:18463–70.
[23] Cho DH, Lee SY, Shin DW, Hwang DS, Lee YM. Swelling agent adopted decal transfer method for membrane electrode assembly fabrication. J Power Sources 2014;258:272–80.
[24] Debe MK. Electrocatalyst approaches and challenges for automotive fuel cells. Nature 2012;486:43–51.
[25] Passalacqua E, Lufrano F, Squadrito G, Pattia A, Giorgi L. Influence of the structure in low-Pt loading electrodes for polymer electrolyte fuel cells. Electrochim Acta 1998;43:3665–73.
[26] Saha MS, Gulla AF, Allen RJ, Mukerjee S. High performance polymer electrolyte fuel cells with ultra-low Pt loading electrodes prepared by dual ion-beam assisted deposition. Electrochim Acta 2006;51:4680–92.
[27] Suzuki T, Tsushima S, Hirai S. Effects of Nafion® ionomer and carbon particles on structure formation in a proton-exchange membrane fuel cell catalyst layer fabricated by the decal-transfer method. Int J Hydrogen Energy 2011;36:12361–9.
[28] Greszler TA, Caulk D, Sinha P. The impact of platinum loading on oxygen transport resistance. J Electrochem Soc 2012;159:F831–40.
[29] Cho YH, Jung N, Kang YS, Chung DY, Lim JW, Choe H, et al. Improved mass transfer using a pore former in cathode catalyst layer in the direct methanol fuel cell. Int J Hydrogen Energy 2012;37:11969–74.
[30] Owejan JP, Owejan JE, Gu W. Impact of platinum loading and catalyst layer structure on PEMFC performance. J Electrochem Soc 2013;160:F824–33.
[31] Shukla S, Domican K, Karan K, Bhattacharjee S, Secanell M. Analysis of low platinum loading thin polymer electrolyte fuel cell electrodes prepared by inkjet printing. Electrochim Acta 2015;156:289–300.
[32] Uchida M, Aoyama M, Eda M, Ohta M. New preparation method for polymer-electrolyte fuel cells. J Electrochem Soc 1995;142:463–8.
[33] Shin SJ, Lee JK, Ha HY, Hong SA, Chun HS, Oh IH. Effect of the catalytic ink preparation method on the performance of polymer electrolyte membrane fuel cells. J Power Sources 2002;106:146–52.
[34] Fernandez R, Ferreira-Aparicio P, Daza L. PEMFC electrode preparation: influence of the solvent composition and evaporation rate on the catalytic layer microstructure. J Power Sources 2005;151:18–24.
[35] Yang TH, Yoon YG, Park GG, Lee WY, Kim CS. Fabrication of a thin catalyst layer using organic solvents. J Power Sources 2004;127:230–3.
[36] Chisaka M, Daiguji H. Effect of organic solvents on catalyst layer structure in polymer electrolyte membrane fuel cells. J Electrochem Soc 2009;156:B22–6.
[37] Therdthianwong A, Ekdharmasuit P, Therdthianwong S. Fabrication and performance of membrane electrode assembly prepared by a catalyst-coated membrane method: effect of solvents used in a catalyst ink mixture. Energy Fuel 2010;24:1191–6.
[38] Wang W, Chen S, Li J, Wang W. Fabrication of catalyst coated membrane with screen printing method in a proton exchange membrane fuel cell. Int J Hydrogen Energy 2015;40:4649–58.
[39] Wilson MS. Membrane catalyst layer for fuel cells. US Patent 5,211,984, May 1993.
[40] Okamoto T, Tanaka I, Kato H, Kawagoe N, Yamamoto A. Method for producing electrode unit for fuel cells. US Patent 5,752,988, May 1998.
[41] Chisaka M, Daiguji H. Effect of glycerol on micro/nano structures of catalyst layers in polymer electrolyte membrane fuel cells. Electrochim Acta 2006;51:4828–33.

[42] Paul DK, Fraser A, Karan K. Towards the understanding of proton conduction mechanism in PEMFC catalyst layer: conductivity of adsorbed Nafion films. Electrochem Commun 2011;13:774–7.
[43] Paul DK, Karan K, Docoslis A, Giorgi JB, Pearce J. Characteristics of self-assembled ultrathin Nafion films. Macromolecules 2013;46:3461–75.
[44] Modestino MA, Paul DK, Dishari S, Petrina SA, Allen FI, Hickner MA, et al. Self-assembly and transport limitations in confined Nafion films. Macromolecules 2013;46:867–73.
[45] Dishari SK, Hickner MA. Confinement and proton transfer in Nafion thin films. Macromolecules 2013;46:413–21.
[46] Borges DD, Franco AA, Malek K, Gebel G, Mossa S. Inhomogeneous transport in model hydrated polymer electrolyte supported ultrathin films. ACS Nano 2013;7:6767–73.
[47] Paul DK, Karan K. Conductivity and wettability changes of ultrathin films subjected to thermal annealing and liquid water exposure. J Phys Chem C 2014;118:1828–35.
[48] Loppinet B, Gebel G. Small-angle scattering study of perfluorosulfonated ionomer solutions. J Phys Chem B 1997;101:1884–92.
[49] Johnston CM, Lee KS, Rockward T, Labouriau A, Mack N, Kim YS. Impact of solvent on ionomer structure and fuel cell durability. ECS Trans 2009;25:1617–22.
[50] Welch C, Labouriau A, Hjelm R, Orler B, Johnston C, Kim YS. Nafion in dilute solvent systems: dispersion or solution? ACS Marco Lett 2012;1:1403–7.
[51] Jung CY, Kim TH, Yi SC. Ultrahigh PEMFC performance of a thin-film, dual-electrode assembly with tailored electrode morphology. ChemSusChem 2014;7:466–73.
[52] Kim YS, Welch CF, Mack NH, Hjelm RP, Orler EB, Hawley ME, et al. Highly durable fuel cell electrodes based on ionomers dispersed in glycerol. Phys Chem Chem Phys 2014;16:5927–32.
[53] Kim YS, Welch CF, Hjelm RP, Mack NH, Labouriau A, Orler EB. Origin of toughness in dispersion-cast Nafion membranes. Macromolecules 2015;48:2161–72.
[54] Kundu S, Fowler MW, Simon LC, Grot S. Morphological features (defects) in fuel cell membrane electrode assemblies. J Power Sources 2006;157:650–6.
[55] a)Hizir FE, Ural SO, Kumbur EC, Mench MM. Characterization of interfacial morphology in polymer electrolyte fuel cells: micro-porous layer and catalyst layer surfaces. J Power Sources 2010;195:3463–71.
b)Jung CY, Yi SC. Improved polarization of mesoporous electrodes of a proton exchange membrane fuel cell using N-methyl-2-pyrrolidinone. Electrochim Acta 2013;113:37–41.
[56] Lee KS, Jeong MH, Lee JS, Pivovar BS, Kim YS. Optimizing end-group cross-linkable polymer electrolytes for fuel cell applications. J Membr Sci 2010;352:180–8.
[57] Carter RN, Kocha SS, Wagner FT, Fay M, Gasteiger HA. Artifacts in measuring electrode catalyst area of fuel cells through cyclic voltammetry. ECS Trans 2007;11:403–10.
[58] Soboleva T, Zhao X, Malek K, Xie Z, Navessin T, Holdcroft S. On the micro-, meso-, and macroporous structures of polymer electrolyte membrane fuel cell catalyst layers. ACS Appl Mater Interfaces 2010;2:375–84.
[59] Xie Z, Navessin T, Zhao X, Adachi M, Holdcroft S, Mashio T, et al. Nafion ionomer aggregation and its influence on proton conduction and mass transport in fuel cell catalyst layer. ECS Trans 2008;16:1811–6.
[60] Schlick S, Gebel G, Pineri M, Volino F. ^{19}F NMR spectroscopy of acid Nafion membranes and solutions. Macromolecules 1991;24:3517–21.
[61] Ghassemzadeh L, Kreuer KD, Maier J, Muller K. Chemical degradation of Nafion membranes under mimic fuel cell conditions as investigated by solid-state NMR spectroscopy. J Phys Chem C 2010;114:14635–45.
[62] Ngo TT, Yu TL, Lin HL. Nafion-based membrane electrode assemblies prepared from catalyst inks containing alcohol/water solvent mixtures. J Power Sources 2013;238:1–10.
[63] Uchida M, Aoyama Y, Eda N, Ohta A. Investigation of the microstructure in the catalyst layer and effects of both perfluorosulfonate ionomer and PTFE-loaded carbon on the catalyst layer of polymer electrolyte fuel cells. J Electrochem Soc 1995;142:4143–9.